Requirements for Osmosensing and Osmotic Activation of Transporter ProP from *Escherichia coli*†

Kathleen I. Racher, Doreen E. Culham, and Janet M. Wood*

Department of Microbiology and Guelph−Waterloo Centre for Graduate Work in Chemistry and Biochemistry, University of Guelph, Guelph, Ontario N1G 2W1, Canada

Received October 4, 2000; Revised Manuscript Received April 17, 2001

ABSTRACT: Transporter ProP of *Escherichia coli*, a solute-H^+ symporter, can sense and respond to osmotic upshifts imposed on cells, on membrane vesicles, or on proteoliposomes that incorporate purified ProP-$(His)_6$. In this study, proline uptake catalyzed by ProP was used as a measure of its osmotic activation, and the requirements for osmosensing were defined using the proteoliposome system. The initial rate of proline uptake increased with decreasing external pH and increasing $\Delta\Psi$, lumen negative. Osmotic upshifts increased $\Delta\Psi$ by concentrating lumenal K^+, but osmotic activation of ProP could be distinguished from this effect. Osmotic activation of ProP resulted from changes in V_{max}, though osmotic shifts also increased the K_M for proline. Osmotic activation could be described as a reversible, osmotic upshift-dependent transition linking (at least) two transporter protein conformations. No correlation was observed between ProP activation and the position of the anions of activating sodium salts within the Hofmeister series of solutes. Both the magnitude of the osmotic upshift required to activate ProP and the ProP activity attained were similar for membrane-impermeant osmolytes, including NaCl, glucose, and PEG 600. The membrane-permeant osmolytes glycerol, urea, PEG 62, and PEG 106 failed to activate ProP. Two poly(ethylene glycol)s, PEG 150 and PEG 200, were membrane-permeant and did not cause liposome shrinkage, but they did partially activate ProP-$(His)_6$.

Living cells control their hydration and/or volume by modulating cytoplasmic osmolality. In most cases, the preferred osmoregulatory mechanism is the accumulation and release of organic osmolytes that are preferentially excluded from macromolecular surfaces (e.g., polyols, betaines) (*1*−*5*). In bacteria, osmoprotectant transporters mediate the uptake of exogenous compounds (osmoprotectants) in response to osmotic upshifts, and mechanosensitive channels mediate the release of cytoplasmic solutes in response to osmotic downshifts (*1*, *6*−*8*). Our goal is to understand the mechanisms by which cells sense changes in extracellular osmolality, thereby modulating the activities of osmoregulatory transporters.

Transporter ProP of *Escherichia coli* mediates the accumulation of several structurally related organic solutes (e.g., proline, glycine betaine, ectoine) in response to increased extracellular osmolality (*9*, *10*). The *proP* sequence predicts a 500 amino acid protein with 12 membrane-spanning domains that belongs to the major facilitator superfamily of transporter proteins (*11*) (Figure 1A). We purified a histidine-tagged ProP variant, ProP-$(His)_6$, and reconstituted it with *E. coli* lipid (*12*). In the resulting proteoliposomes, ProP-$(His)_6$ mediated proline uptake only if a membrane potential (lumen negative) and an osmotic upshift were imposed. Thus, ProP alone is able to sense increased extraliposomal osmolality, transduce the resulting signal, and respond by modulating cytoplasmic composition. Two other transporters, BetP of *Corynebacterium glutamicum* (*13*) and OpuA of *Lactococcus lactis* (*14*), have now been purified, reconstituted, and shown to both sense and respond to osmotic upshifts in vitro.

Proteoliposomal ProP-$(His)_6$ is inactive in the absence of an osmotic upshift (*12*). It is a proton-solute symporter whose activity requires a membrane potential ($\Delta\Psi$)[1] and is further stimulated by a proton gradient (ΔpH) [(*10*, *12*) and data presented herein]. Figure 1B shows our current model linking osmosensing with proline transport catalyzed by ProP. In this study, we offer evidence that osmosensing involves at least two conformations of ProP, inactive ($ProP^I$) and active ($ProP^A$). Additional conformations of ProP may exist, but we confine this discussion to two states for simplicity. Our data indicate that both V_{max} and K_M for proline are affected by osmotic shifts ($\Delta\Pi$). The transport of substrate is the response to osmotic activation. The proposed transport mechanism is based on that validated for other secondary transporters such as the lactose permease (*15*). Since neither the ratio of protons to proline transported nor the order of substrate binding has been determined, those elements of the model are arbitrary.

† This work was supported by a research grant awarded to J.M.W. by the Natural Sciences and Engineering Research Council of Canada.

* Address correspondence to this author at the Department of Microbiology, University of Guelph, Guelph, Ontario N1G 2W1, Canada. Telephone: 519 824 4120, ext. 3866; FAX: 519 837 1802; Email: jwood@uoguelph.ca.

[1] Abbreviations: $\Delta\Pi$, osmotic upshift; $\Delta\Psi$, membrane potential; MOPS, 4-morpholinopropanesulfonic acid; EDTA, ethylenediaminetetraacetic acid; diS-C_3-(5), 3,3′-dipropylthiadicarbocyanine; PEG, poly(ethylene glycol).

10.1021/bi002331u CCC: $20.00
Published on Web 05/15/2001

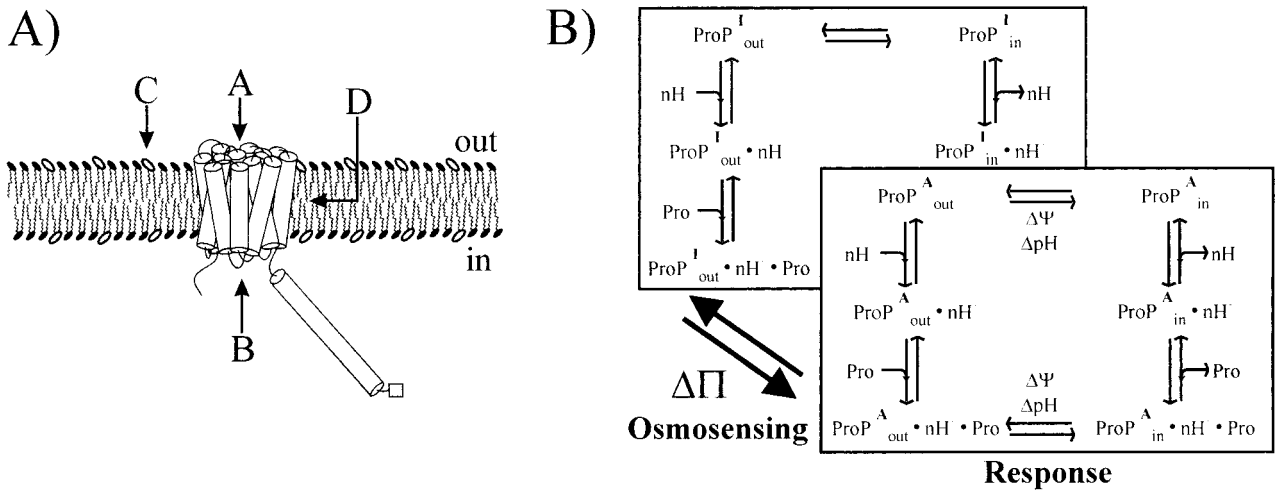

FIGURE 1: Models of (A) ProP-$(His)_6$ in the membrane and (B) ProP-$(His)_6$ activation and transport mechanism. ΔΠ, osmotic upshift; out, periplasm or extraproteoliposomal medium; in, cytoplasm or proteoliposome lumen; pro, proline; ΔΨ, membrane potential; ΔpH, transmembrane pH gradient. (A) The arrows point to regions of ProP-$(His)_6$ and the membrane through which osmotic shifts may be sensed. The helicies of ProP-$(His)_6$ in (A) are represented as cylinders and are drawn to scale with the lipid molecules. The histidine-tag at the C-terminus of ProP-$(His)_6$ is indicated by a gray box. The C-terminal domain is α-helical (*25*), and its presence in the cytoplasm has been verified (Culham, Racher, and Wood, unpublished data). The membrane orientation of proteoliposome-based ProP-$(His)_6$ is currently under investigation. (B) The inactive and active conformations of ProP are represented by $ProP^I$ and $ProP^A$, respectively. Both K_M and V_{max} for proline uptake are affected by osmotic shifts (see Figure 4).

No change in ProP protein structure has yet been correlated with osmosensing. As a result, we currently measure changes in the catalytic activity of ProP in response to ΔΠ and infer the proportions of $ProP^A$ and $ProP^I$ from the measured transport rate. This approach is only valid if other effects of ΔΠ on the transport response can be eliminated or taken into account (*16*). For example, increasing osmolality may affect substrate binding by ProP and the transport driving forces, ΔΨ and ΔpH. Therefore, our initial objective was to define and control the dependence of a number of transport assay variables on osmotic shifts.

Having addressed those issues, we would like to understand what triggers the conformational change that activates ProP. Osmotic shifts have multiple effects on the environments of proteins integrated in cytoplasmic or proteoliposomal membranes (*1*), including (see Figure 1A): (A) changes in the periplasm or extraliposomal solvent, detectable by protein domains exposed to that compartment; (B) changes in the cytoplasm or liposome lumen, detectable by protein domains exposed to that compartment; (C) changes in the membrane due to membrane-excluded osmolytes, detectable by the membrane-integral protein domain or protein domains that interact with the membrane surface; (D) changes in the intramembrane solvent due to membrane-permeant osmolytes, detectable by the membrane-integral protein domain; or (E) concerted changes involving more than one of these solvent effects. The critical change(s) detected by osmosensors may be either transient (occurring on the time scale of osmotically induced transmembrane water flux) or sustained postflux (occurring on a much longer time scale). Since water flux across membranes in response to osmotic shifts [complete within milliseconds (*17, 18*)] occurs on a much shorter time scale than ProP activation [complete within minutes, at least in intact cells (*19*)], our working hypothesis is that ProP senses changes that are sustained after osmotically induced water flux. We would like to know which consequences of osmotic upshifts are sensed by ProP.

Although osmosensing through direct sensor−solvent interaction has been deemed unlikely, it is not impossible (*1*). For example, studies designed to probe the role of hydration changes in biological processes have revealed that osmotic stress can induce changes in macromolecular structures and interactions (*16, 20, 21*). By analogy, changes in ProP conformation could result directly from changes in water activity in one or more of the solvent phases to which it is exposed. Osmosensing would simply connect a dehydration-associated conformational change of the sort commonly observed with other systems to a specific homeostatic response. Alternatively, the crucial conformational change from $ProP^I$ to $ProP^A$ may be induced indirectly via changes in its membrane environment. The principles relating protein conformation to solvent composition also apply to membranes (*22*). Although many membrane properties can be influenced by solvent composition, the relationships linking particular membrane properties with solvent osmolality, per se, have not been delineated (*1*).

Experimenters have routinely employed only a limited variety of inorganic and organic osmolytes in attempts to distinguish bacterial responses to specific solutes from osmoregulatory responses (*1*). For example, osmotic activation of transporter ProP can be achieved with either NaCl or sucrose as osmolyte (*12*). Rigorous assessment of the requirements for ProP activation requires in-depth study using a broader osmolyte range and a simpler experimental system than intact bacteria or cytoplasmic membrane vesicles. We have used the proteoliposome system to begin such a study. For example, solutes can be arranged in the Hofmeister series from the most kosmotropic (water structure-making) to the most chaotropic (water structure-breaking) (*23*). Relatively kosmotropic solutes decrease protein solubility (salting-out effect), increase protein denaturation temperatures, alter enzyme activities, and favor lipid bilayer phases with increased headgroup packing (*24*). Chaotropes have the opposite effects. We have examined the abilities of both kosmotropic and chaotropic solutes to activate ProP. Studies

of the bacterial osmotic stress response have routinely included membrane-permeant osmolytes, and generally those osmolytes have failed to induce or activate osmoregulatory responses (*1*). For example glycerol, which is membrane-permeant for *E. coli*, activates ProP only transiently in intact cells (*9*) and fails to activate in cytoplasmic membrane vesicles (*19*) or proteoliposomes (*12*). We have now explored the relationship between proteoliposome shrinkage and ProP activation by using poly(ethylene glycol)s (PEGs) as osmolytes with systematically variable molecular sizes and membrane permeabilities.

EXPERIMENTAL PROCEDURES

Materials. *E. coli* phospholipids (polar lipid extract, acetone/ether washed) and dodecyl β-D-maltoside were purchased from Avanti Polar Lipids, Inc. (Alabaster, AL). Mono-, di-, and triethylene glycols as well as all higher molecular weight poly(ethylene glycol)s were purchased from Fluka (Oakville, ON). Calcein was purchased from Sigma (Oakville, ON).

Expression, Purification, and Reconstitution of ProP-(His)$_6$. The *proP*−*(his)*$_6$ gene was inserted behind the arabinose-inducible P_{BAD} promoter in plasmid pBAD24 to create plasmid pDC80. Plasmid pDC80 was transformed into *E. coli* strain WG350 [F$^-$ *trp lacZ rpsL thi* Δ(*putPA*)*101* Δ(*proU*)*600* Δ(*proP-melAB*)*212*], creating strain WG710. Culham et al. (*25*) described the bacterial strains and the construction of pDC80. Strain WG710 was grown in MOPS-based minimal medium (*26*) supplemented with 9.5 mM NH_4Cl, 4% (w/v) glycerol, 245 μM L-tryptophan, and 1 μg/mL thiamin hydrochloride. The culture was grown at 37 °C with shaking to an optical density (at 600 nm) of 1.0; then arabinose was added to a final concentration of 2% (w/v). The culture was grown for an additional 2 h and then harvested by centrifugation and washed with 0.1 M potassium phosphate buffer, pH 7.4. Preparation of membrane vesicles and the subsequent purification and reconstitution of ProP-(His)$_6$ into *E. coli* lipid liposomes were described in Racher et al. (*12*) based on the procedure of Jung et al. (*27*).

Transport Measurements. All assay buffers contained 0.1 M sodium phosphate and 0.5 mM Na-EDTA. Assay buffers containing osmolyte were prepared by mixing 0.1 M dibasic sodium phosphate, 0.5 mM Na-EDTA plus osmolyte and 0.1 M monobasic sodium phosphate, 0.5 mM Na-EDTA plus osmolyte until the desired pH was reached (pH 6.4 unless otherwise noted). It was necessary to prepare the buffers in this way as the pK_a of phosphate buffer is strongly dependent on ionic strength (*28*). The osmolality of all solutions was measured with a vapor pressure osmometer (Wescor, Logan, UT). Each osmotic upshift reported in this paper is the difference between the measured osmolality of the relevant transport assay buffer and the measured osmolality of the buffer internal to the proteoliposomes.

Immediately before use, proteoliposomes (prepared in 0.1 M potassium phosphate, pH 7.4, 0.5 mM Na-EDTA) were extruded 20 times through a 19 mm Nucleopore polycarbonate filter (Costar, Cambridge, MA) with a pore size of 0.4 μm. For the transport assays, 3 μL of proteoliposomes (0.2 mg/mL protein, 60 mg/mL lipid) was diluted 200-fold into the sodium phosphate-based assay buffer (to create an outwardly directed potassium gradient). The buffer was supplemented with 2 mM β-mercaptoethanol, 5 mM $MgSO_4$, 0.1 μM valinomycin, and L-[^{3}H]-proline. The proline concentration varied as specified, and the specific radioactivity was adjusted as required in the range 25−700 Ci/mol. Aliquots (180 μL) were withdrawn at 30, 60, and 90 s, or aliquots (140 μL) were withdrawn at 20, 40, 60, and 80 s. Each aliquot was added to 2.5 mL of quench buffer (0.1 M potassium phosphate, pH 6.0, 0.1 M LiCl) and filtered through a 0.22 μm nitrocellulose filter. Each filter was washed once more with 2.5 mL of quench buffer and then placed in 5 mL of Beckman Ready-Protein scintillation cocktail for counting. Experiments were performed twice; error bars reported for the activity data represent the standard error of the mean of at least three replicate measurements from a representative experiment.

The ability of proteoliposomes to maintain a membrane potential over the time course of the transport assay was measured using the membrane potential-sensitive fluorescent dye diS-C_3-(5) (*29*). Proteoliposomes were diluted 200-fold into 0.1 M sodium phosphate (pH 6.4) containing 0.3 M NaCl and 1 μM diS-C_3-(5). Valinomycin was added to 0.1 μM, and fluorescence was measured as described by Racher et al. (*12*). The measured membrane potential was constant for at least 2 min (data not shown).

Calculations Related to the Applied Membrane Potential. Since valinomycin elevates the membrane permeability of K^+ well above that of all other ions, the magnitude of the membrane potential (ΔΨ) is set only by the concentrations of K^+ on either side of the proteoliposomal membrane. Therefore, values of ΔΨ reported in this paper have been calculated using the equation:

$$\Delta\Psi = \frac{-RT}{F} \ln \frac{[K^+]_{in}}{[K^+]_{out}} \quad (1)$$

where R is the gas constant, T is the temperature (in degrees kelvin), F is the Faraday constant, and $[K^+]_{in}$ and $[K^+]_{out}$ are the potassium concentrations in the proteoliposome lumen and the external medium, respectively. If the proteoliposomes act as ideal osmometers, they shrink as the osmolality of the assay buffer increases, and $[K^+]_{in}$ increases linearly according to the equation:

$$[K^+]_{in} = [K^+]_{in}{}^{o} (\Pi/\Pi^o) \quad (2)$$

where $[K^+]_{in}$ is the lumenal potassium concentration post-shift, $[K^+]_{in}{}^{o}$ is the lumenal potassium concentration prior to osmotic upshift, and Π^o and Π are the osmotic pressures before and after the osmotic upshift, respectively. In these experiments, $[K^+]_{in}{}^{o}$ was 178 mM as measured by titrating 0.1 M KH_2PO_4 with 0.1 M K_2HPO_4 until a pH of 7.4 was reached. For some experiments, the value of ΔΨ was kept constant, despite applied osmotic upshifts, by adding KCl to the assay buffer. The amount of KCl necessary was calculated using eqs 1 and 2 and measured values for proteoliposome shrinkage, described below.

Fluorescence Assay To Measure Solute Permeability of E. coli Lipid Liposomes. Liposomes were prepared with *E. coli* phospholipid and stored as described by Racher et al. (*12*). Calcein was prepared at a concentration of 10 mM in

0.1 M potassium phosphate and the pH adjusted to 7.4 using saturated KOH. Liposomes were recovered by centrifugation for 20 min at 175000*g* in a Beckman Airfuge, resuspended in the calcein solution, and then extruded as described above (see *Transport Measurements*). External calcein was washed away from the liposomes by repeated centrifugation and resuspension in calcein-free 0.1 M potassium phosphate buffer, pH 7.4. Fluorescence measurements were made with an Hitachi F-2000 Fluorescence Spectrophotometer at an excitation wavelength of 495 nm and an emission wavelength of 520 nm (slit width of 10 nm). Osmotic upshifts were imposed by diluting 5 μL of calcein-loaded liposomes (20 mg/mL lipid) into 1.5 mL of 0.1 M sodium phosphate (pH 6.4) with or without added osmolyte in a 4 mL cuvette. Samples were mixed by inversion and held at room temperature for exactly 1 min before the fluorescence was measured. Each fluorescence experiment was performed at least twice; the error bars reported for the fluorescence data represent the standard error of the mean of three replicate measurements from a representative experiment.

The possibility that membrane-permeant solutes would interfere in the self-quenching of calcein was tested by comparing the fluorescence of calcein (at the partially self-quenched concentration of 10 mM) in sodium phosphate buffer with or without the solute. Due to the strong inner filter effect with calcein, fluorescence was measured in a triangular cuvette (for front-face illumination) at an excitation wavelength of 420 nm and an emission wavelength of 520 nm. The calcein fluorescence was unchanged in the presence or absence of 0.8 M PEG 200, 0.7 M glycerol, or 0.4 M ethylene glycol.

RESULTS

pH Dependence of ProP-(His)$_6$ Activity in Proteoliposomes. Since ProP is an enzyme and a proton symporter, the extraproteoliposomal pH, the lumenal pH, and the magnitude and direction of the transmembrane proton gradient (ΔpH) are all expected to affect the measured activity of ProP-(His)$_6$. ProP-(His)$_6$ activity was measured as a function of assay buffer pH at a constant lumenal pH of 7.4 and a constant osmotic upshift of 0.56 mol/kg (imposed with NaCl). As expected, the proline uptake activity of ProP-(His)$_6$ increased as the pH of the assay buffer decreased (Figure 2A). Concentration of the potassium phosphate buffer (pH 7.4) from 0.1 to 0.5 M does not change the buffer pH; therefore, we expect the lumenal pH to remain constant as the proteoliposomes shrink in response to osmotic upshifts. The pH of the external buffer was set at 6.4 for all subsequent assays, giving a ΔpH of 1 unit.

The Membrane Potential ($\Delta\Psi$) and ProP-(His)$_6$ Activity: Relationship to Proteoliposome Shrinkage. ProP-(His)$_6$ activity increased with increasing membrane potential ($\Delta\Psi$) when a constant osmotic upshift (0.56 mol/kg) was imposed with NaCl (Figure 2B). This direct dependence of transport activity on the magnitude of $\Delta\Psi$ is a common feature of electrogenic transport (*13, 30*). When an osmotic upshift is imposed on proteoliposomes with a membrane-impermeant solute, water diffuses out of the lumen, shrinking the proteoliposome and concentrating the lumenal contents (in this case 0.1 M potassium phosphate, pH 7.4). According to eq 1 (Experimental Procedures), increasing the lumenal potassium concentration ($[K^+]_{in}$) will also increase the magnitude of the membrane potential ($\Delta\Psi$). As expected, an increase in $\Delta\Psi$ could be observed with the fluorescent dye diS-C$_3$-(5) when osmotic upshifts were imposed on the proteoliposomes with membrane-impermeant solutes (data not shown).

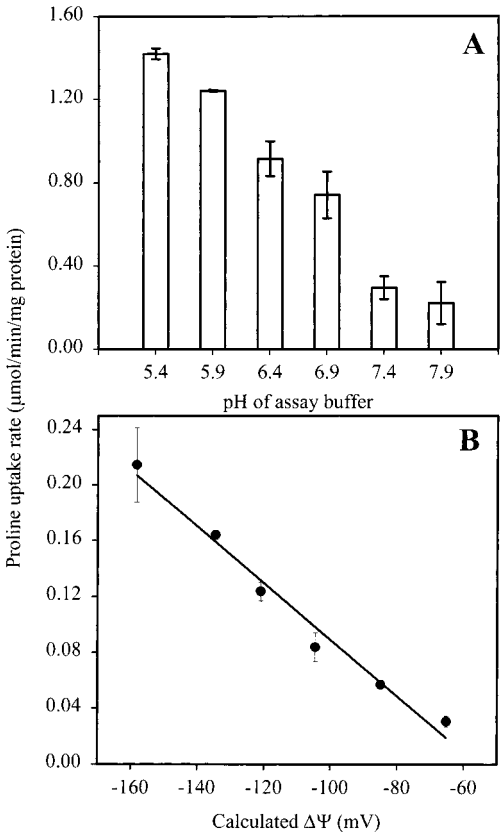

FIGURE 2: Dependence of ProP-(His)$_6$ activity on the extraproteoliposomal pH and the applied membrane potential. Proteoliposomes (internal pH of 7.4) were diluted 200-fold into 0.1 M sodium phosphate buffer supplemented with NaCl to impose an osmotic upshift of 0.56 mol/kg. Proline uptake was measured as described under Experimental Procedures. (A) Proteoliposomes were diluted into buffers of the indicated pH, containing 200 μM proline. (B) Proteoliposomes were diluted into pH 6.4 buffers supplemented with K^+ to adjust the membrane potential. The concentration of proline was 40 μM for this experiment.

The fluorescence of calcein-loaded liposomes was monitored to measure the proteoliposome shrinkage that resulted when osmotic upshifts were imposed with various osmolytes (see Experimental Procedures). Calcein was used in this assay as its fluorescence is self-quenched at concentrations above 1 mM (*31*) and its fluorescence is insensitive to pH in the range 5−9 (*32*). Liposomes were used because proteoliposomes and liposomes prepared from *E. coli* phospholipid are similar in size (mean diameter approximately 175 nm) and structural response to osmotic shifts (*33*). Liposomes were loaded with calcein at a concentration sufficient to initiate self-quenching and diluted into buffers of increasing osmolality (Figure 3). As they shrank, the internal calcein concentration increased, thereby increasing self-quenching and decreasing the measured fluorescence. The osmolytes NaCl and glucose gave identical results, and the correlation between fluorescence and osmolality was linear for osmotic upshifts from 0 to 0.6 mol/kg. NaCl and glucose were chosen since they are known to be membrane-impermeant (at least

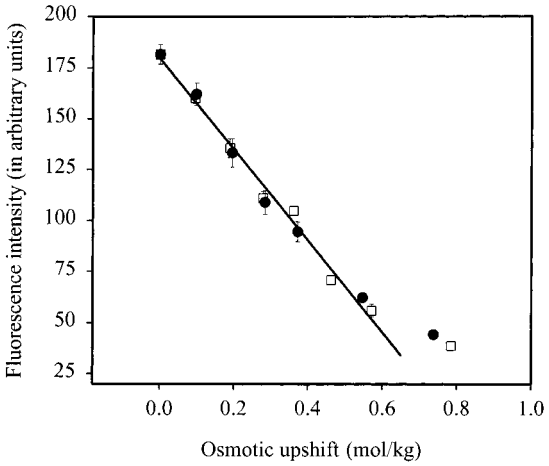

FIGURE 3: Measurement of liposome shrinkage using calcein. Osmotic upshifts were imposed on calcein-loaded liposomes by a 300-fold dilution into 0.1 M sodium phosphate buffer adjusted to the indicated osmolality with either NaCl (closed circles) or glucose (open squares). Fluorescence measurements were performed as described under Experimental Procedures.

in the time frame of this assay) (*34*).

The dependence of ProP-$(His)_6$ activity on osmotic upshift was determined with $\Delta\Psi$ either kept constant at −137 mV (by adding extraproteoliposomal KCl, as described under Experimental Procedures, Figure 4A, closed circles) or allowed to increase between −137 and −168 mV as a consequence of osmotic upshifts applied with NaCl (Figure 4A, open circles). The effect on $\Delta\Psi$ of increasing osmotic upshift with a membrane-impermeant osmolyte is depicted in the inset to Figure 4A. Note that the concentrations of extraproteoliposomal KCl added to control $\Delta\Psi$ were between 0.1 and 4 mM, concentrations too low to contribute significantly to the assay buffer osmolality. Clamping the voltage reduced the proline uptake rate observed after large osmotic upshifts, as expected. The requirement for osmotic activation of ProP-$(His)_6$ at constant $\Delta\Psi$ nevertheless remained evident. ProP was also activated when PEG 600 was employed as activating osmolyte at constant membrane potential (−137 mV, Figure 4B). All data described in subsequent sections of this paper were obtained by imposing a constant $\Delta\Psi$ in this way unless otherwise noted.

Effects of Osmotic Upshifts on V_{max} and K_M(Proline) for ProP-$(His)_6$. The K_M and V_{max} values for reconstituted ProP-$(His)_6$ were determined in proteoliposomes that were exposed to osmotic upshifts of increasing magnitude (NaCl as osmolyte). Both V_{max} and K_M increased with increasing osmotic upshift at constant pH gradient and membrane potential (−147 mV) (Figure 5). The catalytic efficiency of the enzyme as indicated by V_{max}/K_M remained essentially constant (see inset to Figure 5B), but proline uptake activity did increase as a function of osmotic upshift when proline concentration was held relatively high and constant (e.g., 200 μM proline, Figure 4). These results are reflected in the kinetic scheme represented in Figure 1B.

The Osmotic Activation of ProP-$(His)_6$ Is Reversible. The reversibility of ProP activation was tested by first subjecting proteoliposomes to an osmotic upshift of 0.15 or 0.36 mol/kg with PEG 600 for 30 s, and then diluting them into assay buffer containing valinomycin and proline, with or without PEG 600, to increase, decrease, or cause no further change

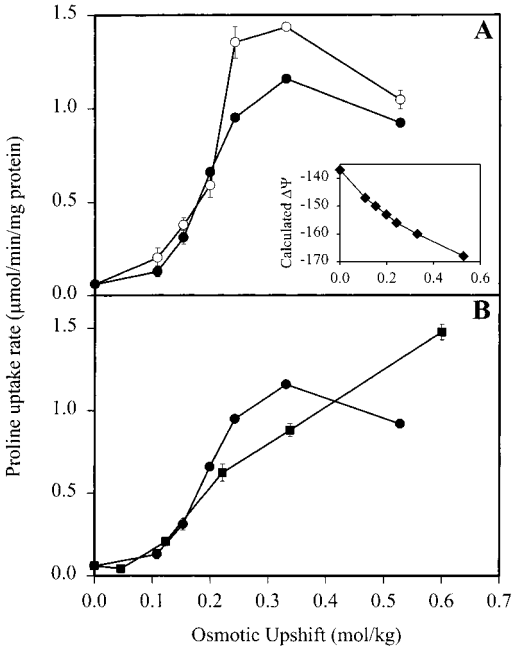

FIGURE 4: Osmotic activation of ProP-$(His)_6$ is independent of osmotic shrinkage-induced membrane potential changes. Proline uptake via ProP-$(His)_6$ was measured by diluting proteoliposomes into 0.1 M sodium phosphate buffer, pH 6.4, containing 200 μM proline as described under Experimental Procedures. (A) ProP-$(His)_6$ activity was measured as a function of osmotic upshift imposed with NaCl. The membrane potential was allowed to vary (open circles), or it was fixed at −137 mV (closed circles). Constant $\Delta\Psi$ was achieved by adjusting the extraproteoliposomal K^+ concentration as indicated by the calculated liposome shrinkage (see eqs 1 and 2). Inset: Expected variation in the membrane potential due to osmotic upshifts imposed with membrane-impermeant osmolytes. $\Delta\Psi$ was calculated using eq 1 (as described under Experimental Procedures). Calculations were based on (proteo)liposomes made in 0.1 M potassium phosphate buffer (pH 7.4) and diluted 200-fold into potassium-free assay buffer. (B) ProP-$(His)_6$ activity was measured as a function of osmotic upshifts imposed with NaCl (circles) or PEG 600 (squares) at a constant $\Delta\Psi$ of −137 mV.

in the osmotic upshift (Figure 6). Final (net) osmotic upshifts were 0, 0.15, or 0.36 mol/kg. The resulting transport activity depended only on the final value of the osmotic upshift, not on the magnitude of the initial upshift. For example, imposing an upshift of 0.36 mol/kg and then a downshift to 0.15 mol/kg gave a transport rate equivalent to a single 0.15 mol/kg upshift. Thus, the transition between inactive and active conformations of ProP ($ProP^I \leftrightarrow ProP^A$) was completely reversible on the time scale of the transport assay as suggested by the model illustrated in Figure 1B.

Dependence of ProP-$(His)_6$ Activation on the Chemical Nature of the Activating Osmolyte. In *E. coli* cells and membrane vesicles, ProP is activated by both sucrose and NaCl (*9*, *19*). Similarly, equal osmotic upshifts imposed on proteoliposomes with glucose or NaCl gave equivalent ProP-$(His)_6$ activity (Table 1). Since both ionic and nonionic solutes activate ProP-$(His)_6$, it is reasonable to assume that the protein is sensing a change in water activity (or some correlate of it) as opposed to the solute itself. In the Hofmeister series, solutes are arranged in a continuum from the most kosmotropic to the most chaotropic. Sodium chloride is considered relatively neutral in its effects on water structure whereas sucrose and glucose are kosmotropes (*23*). We extended these studies with the proteoliposome system, testing the sensitivity of the protein to changes in the

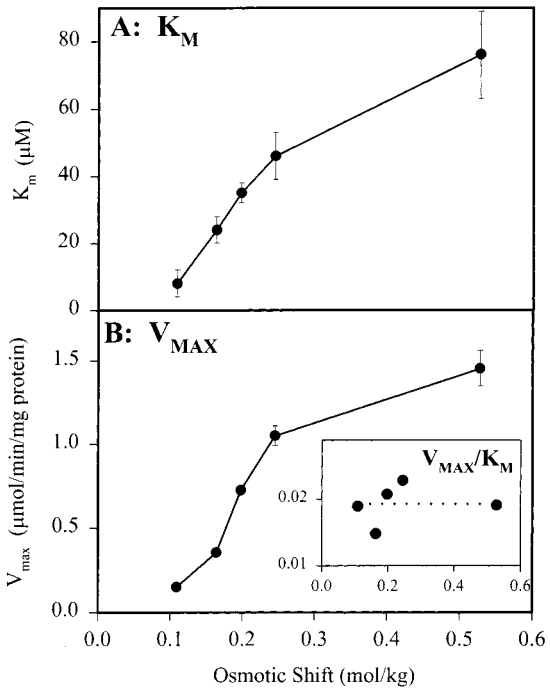

FIGURE 5: Both K_M (panel A) and V_{max} (panel B) for proline uptake via ProP depend on the applied osmotic upshift. Proline uptake via ProP-$(His)_6$ was measured by diluting proteoliposomes (lumenal pH 7.4) into 0.1 M sodium phosphate buffer, pH 6.4, containing [^{3}H]proline (2.4−250 μM) as described under Experimental Procedures. Proteoliposomes were subjected to the indicated osmotic upshifts with NaCl, and the voltage was clamped at −147 mV as described in the text. K_M and V_{max} were computed by fitting the primary data to the Michaelis−Menten equation by nonlinear regression. Inset to panel B: V_{max}/K_M, horizontal dotted line defining the mean value of 0.0193.

properties of water induced by a larger range of solutes. The initial rate of proline uptake via ProP-$(His)_6$ was measured after equal osmotic upshifts (0.35 mol/kg) were imposed with a series of sodium salts that included kosmotropic and chaotropic anions (Figure 7). Solutes used in this experiment were determined to be membrane-impermeant by the fluorescence assay described above. No trend in the activation of ProP-$(His)_6$ was associated with the solute position in the series. Thus, the osmotic activation of ProP appeared to be independent of the exposure of its extraproteoliposomal surface to kosmotropes or chaotropes.

The organic kosmotrope glycerol and the organic chaotrope urea both failed to activate ProP-$(His)_6$ (Table 1). These osmolytes did not inhibit activation of ProP-$(His)_6$ when an osmotic upshift was imposed with glucose in their presence (Table 1). In contrast to the other solutes tested with ProP-$(His)_6$, glycerol and urea did not cause shrinkage of calcein-loaded liposomes. Since membrane-permeant solutes are expected to cross the membrane more slowly than water, osmotic upshifts imposed with these solutes may cause transient shrinkage of (proteo)liposomes. For membrane-permeant solutes, no fluorescence change could be detected 15 s after diluting the calcein-loaded liposomes into osmolyte-containing buffer (the shortest time in which a sample could be mixed and measured). Therefore, according to the calcein assay, the equilibration of solutes deemed membrane-permeant must occur within 15 s [see also (*18*)], and no net proteoliposome shrinkage caused by these solutes was detected in the steady state.

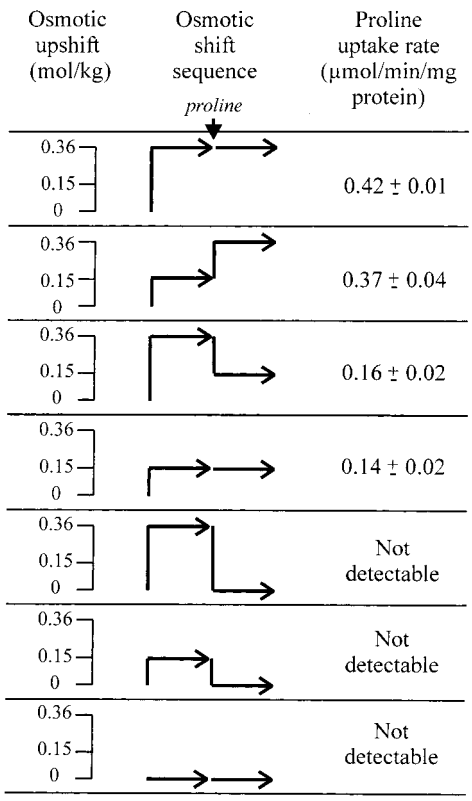

FIGURE 6: ProP-$(His)_6$ activation is reversible. Proteoliposomes were subjected to osmotic upshifts of either 0, 0.15, or 0.36 mol/kg, incubated for 30 s, and then diluted into assay buffer containing valinomycin and proline to initiate transport at final osmotic upshifts of 0, 0.15, or 0.36 mol/kg. Each horizontal arrow represents an incubation time of 30 s. The vertical lines represent osmotic upshifts or downshifts of the magnitude indicated in the first column. Proline uptake rates were measured, using 40 μM proline, as described under Experimental Procedures.

Table 1: Activation of ProP-$(His)_6$ with Various Osmolytes

added osmolyte	[osmolyte] (M)	osmotic upshift (mol/kg)	initial rate of proline uptake [μmol min^{-1} (mg of protein)$^{-1}$]
none	0	0	nd[a]
NaCl	0.2	0.35	0.55 ± 0.01
glucose	0.35	0.35	0.55 ± 0.03
glycerol	0.35	0.35	nd
urea	0.38	0.35	nd
PEG 600	0.15	0.35	0.58 ± 0.07
glycerol + glucose	0.35 & 0.35	0.76	0.60 ± 0.04
urea + glucose	0.38 & 0.35	0.76	0.62 ± 0.03

[a] nd, not detectable.

The fact that glycerol does not activate ProP or other osmosensory proteins [such as BetP (*13*) and OpuA (*35*)] has been taken as evidence that proteoliposome shrinkage is necessary for osmotic activation of these proteins. However, it was necessary to test a wider range of membrane-permeant solutes before the importance of proteoliposomal shrinkage could properly be assessed.

Proteoliposome Shrinkage and ProP-$(His)_6$ Activation. Poly(ethylene glycol)s were selected as osmolytes for these studies because they constitute a chemically similar series of molecules with systematically variable molecular sizes. In addition, their interactions with proteins have been documented (*16*, *36*). The fluorescence of calcein-loaded liposomes was measured at osmotic equilibrium, 1 min after

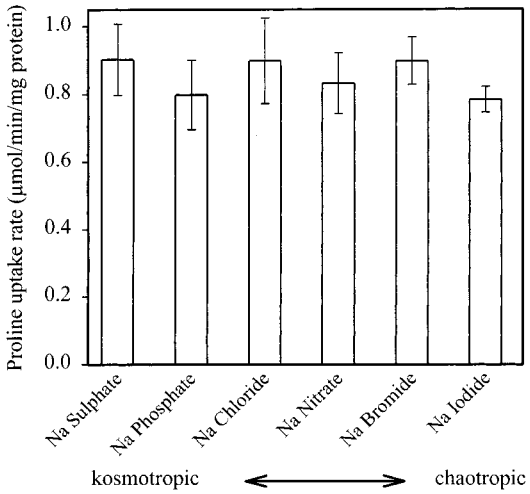

FIGURE 7: Solutes in a typical Hofmeister series activate ProP-$(His)_6$ similarly. The concentrations of the seven solutes were adjusted to each give an osmotic upshift of 0.35 mol/kg. Proline uptake was measured, using 40 μM proline, as described under Experimental Procedures.

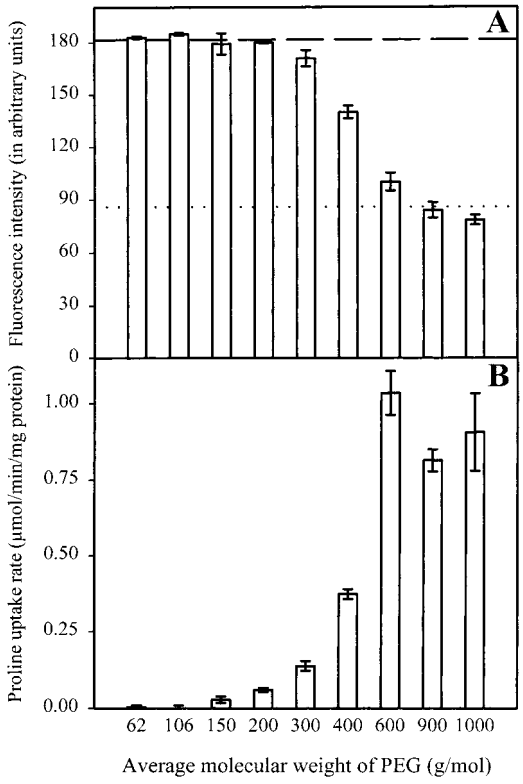

FIGURE 8: Osmotic upshifts imposed with poly(ethylene glycol)s of different molecular weights shrink liposomes (A) and activate ProP-$(His)_6$ (B) to different extents. The osmotic upshift imposed with each PEG solution was 0.35 mol/kg. (A) The fluorescence of calcein-loaded liposomes was measured (after dilution into PEG-containing assay buffer) as described under Experimental Procedures. The dashed and dotted lines represent the fluorescence of liposomes diluted isotonically (no shrinkage) and with an osmotic upshift of 0.35 mol/kg imposed with NaCl, respectively. (B) Proline uptake rates were measured, using 40 μM proline, as described under Experimental Procedures.

their dilution into buffers supplemented with PEGs of differing weight-average molecular mass (Figure 8A). The PEG concentrations were adjusted to give osmotic upshifts of 0.35 mol/kg. The dashed line represents the fluorescence of liposomes diluted into isotonic buffer (no shrinkage), and the dotted line indicates the fluorescence from liposomes diluted into buffer supplemented with an impermeant solute (glucose) to impose an osmotic upshift of 0.35 mol/kg.

PEG 62, PEG 106, and PEG 150 are monodisperse preparations in which each polymer is comprised of 1, 2, or 3 monomer units, respectively. Other poly(ethylene glycol)s are sold as mixtures of varying amounts of different molecular weight polymers whose average is reported as 200, 300, etc. Clearly, PEG 62, PEG 106, PEG 150, and PEG 200 were membrane-permeant on the time scale of this assay whereas PEG 900 and PEG 1000 were membrane-impermeant. The intermediate shrinkage of proteoliposomes caused by PEG 300, PEG 400, and PEG 600 probably resulted from the presence of both membrane-permeant and membrane-impermeant PEG species in these mixtures. This intermediate shrinkage would then occur because the osmotic upshift due to membrane-impermeant species, those that elicit transmembrane water flux and liposome shrinkage, would be smaller than 0.35 mol/kg.

The proline uptake activities of ProP-$(His)_6$ proteoliposomes were determined after an equal osmotic upshift (0.35 mol/kg) was imposed with each PEG as shown in Figure 8B. Upshifts imposed with PEG 600, PEG 900, and PEG 1000 gave similar, high activities. With this large osmotic upshift, the presence of some membrane-permeant species in the PEG 600 mixture did not significantly differentiate its capacity for ProP-$(His)_6$ activation from that of the membrane-impermeant mixtures, PEG 900 and PEG 1000. Osmolytes PEG 300 and PEG 400 were able to partially activate ProP-$(His)_6$, as would be expected if proteoliposome shrinkage were required for ProP-$(His)_6$ activation, and these osmolytes elicited more limited proteoliposome shrinkage than the high-order PEG polymers. As observed with the membrane-permeant osmolytes glycerol and urea (Table 1), PEG 62 and PEG 106 failed to activate ProP-$(His)_6$.

In striking contrast to the behavior of PEG 62 and PEG 106, the fully membrane-permeant osmolytes PEG 150 and PEG 200 were able to partially activate ProP-$(His)_6$. Could it be that PEG 150 and PEG 200 shrink proteoliposomes by a small amount not detectable using the calcein assay and this single PEG concentration? If so, we would expect the liposomes to shrink after exposure to more concentrated PEG 200.

We extended our analysis of the structural and functional consequences of osmotic upshifts imposed with PEG 200 (membrane-permeant) and PEG 600 (predominantly membrane-impermeant) by titrating each osmolyte. The degree of liposome shrinkage caused by increasing osmotic upshifts imposed with each PEG was compared with that due to the membrane-impermeant osmolyte NaCl (Figure 9A). Note that PEG 200 was completely membrane-permeant at all osmolalities tested since it caused no change in fluorescence intensity. In striking contrast, PEG 600 was very close to NaCl in its ability to elicit liposome shrinkage.

The abilities of PEG 200 and PEG 600 to activate ProP-$(His)_6$ were also explored further (membrane potential fixed at -137 mV; Figure 9B). In both cases, ProP-$(His)_6$ activity increased systematically with increasing osmotic upshift, though the extent of activation differed for these two osmolytes. The inset to Figure 9B clearly demonstrates that PEG 200 activated ProP-$(His)_6$ in the absence of proteoliposome shrinkage.

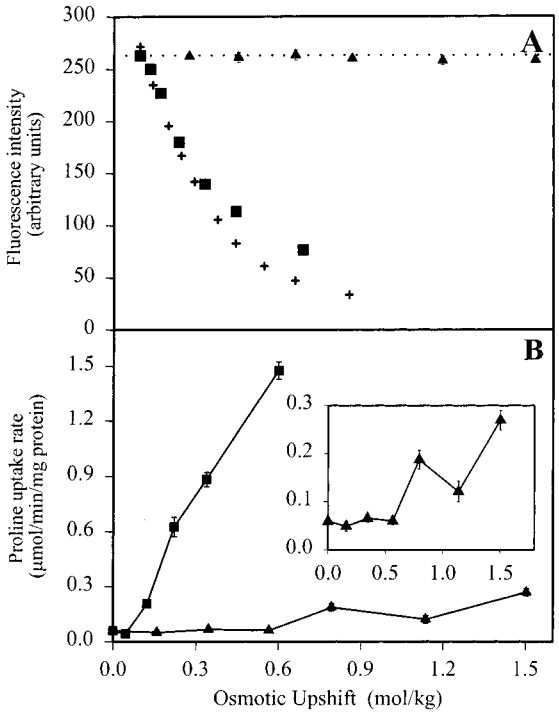

FIGURE 9: ProP-(His)$_6$ activity increases with increasing osmotic upshifts imposed with PEG 200 and PEG 600. (A) The fluorescence of calcein-loaded liposomes was measured as described under Experimental Procedures after dilution into PEG- or NaCl-containing assay buffers of varying osmolalities. PEG 200, triangles; PEG 600, squares; NaCl, plus signs. (B) The proline uptake rates were measured, using 200 μM proline and constant membrane potential (−137 mV), as described under Experimental Procedures. PEG 200, triangles; PEG 600, squares.

DISCUSSION

Our goal is to understand how osmotic upshifts activate ProP. We approach this problem by varying osmolality with different solutes and measuring ProP-mediated uptake of radiolabeled proline into whole bacterial cells, membrane vesicles, or proteoliposomes. Transport activity is then taken as a measure of the proportion of ProP present in the active conformation. Interpretation of the transport data requires, however, that we identify and control those experimental variables that change with osmolality and/or solute chemistry but are unrelated to the activation of the ProP protein. For example, in whole cells and membrane vesicles, the membrane potential is provided by electron flow via the electron-transport chain whose protein components may be adversely affected by the relatively high concentrations of solutes necessary to study osmotic activation of ProP (*37*). In addition, solutes with different chemistries may vary in their effects on proteins (other than ProP) in the *E. coli* membrane.

Purification and reconstitution of ProP have greatly simplified our experimental system, allowing us to rigorously assess the effect of $\Delta\Pi$ on the transport driving forces (ΔpH and $\Delta\Psi$) and to test some of the assumptions in our model of ProP activation and transport (Figure 1B). For example, we have shown that the osmotic activation of ProP is fully reversible (Figure 6), validating both our prediction of an equilibrium between ProP^I and ProP^A (Figure 1B) and the use of proline transport activity as a measure of ProP activation. Unless precautions are taken to fix $\Delta\Psi$, imposition of osmotic upshifts on proteoliposomes increases $\Delta\Psi$ which, in turn, increases ProP-(His)$_6$ activity independent of osmotic activation (Figures 2 and 4). A fluorescence assay was developed to measure proteoliposomal shrinkage after imposition of osmotic upshifts with different solutes (Figure 3). Data obtained with this assay allowed us to control the magnitude of the imposed membrane potential in our activity assays.

Both the K_M for proline and the V_{max} of ProP-(His)$_6$ increased with increasing $\Delta\Pi$, so the catalytic efficiency of the enzyme (V_{max}/K_M) remained essentially constant (Figure 5). Intact bacteria in MOPS medium supplemented with 0.3 M NaCl showed a K_M for proline uptake via ProP of 111 ± 13 μM (*10*), a value comparable to that observed with proteoliposomes under comparable conditions (Figure 5, 0.3 M NaCl, K_M of 78 ± 13 μM). In intact bacteria, the K_i for glycine betaine inhibition of proline uptake via ProP [91 ± 13 μM, measured with 0.3 M NaCl (*10*)] is comparable to the K_M for proline uptake (cited above). This suggests that the transporter has similar K_Ms for the two substrates. Glycine betaine is present in human urine at a controlled level [measured values (mean ± standard deviation) of 78 ± 65 μM (*38, 39*)]. Since this concentration is high in relation to the observed K_M range for ProP (Figure 5), transporter activity would be expected to increase with increasing urine osmolality. On the basis of these data, k_{cat} for ProP-(His)$_6$ increased 10-fold from 0.14 to 1.4 s^{-1} as the imposed osmotic upshift increased from 0.11 to 0.53 mol/kg [these values are based on the assumption that all proteoliposomal ProP-(His)$_6$ is equally active]. Further analyses of the impact of osmolality on proline binding to ProP will be required to assess whether the effect of osmolality on K_M corresponds quantitatively to this effect on k_{cat}. In contrast to this behavior of ProP-(His)$_6$, a constant K_M value with increasing osmolality has been observed for osmosensor OpuA (*35*).

Experimenters have routinely used the similarity of responses to various ionic and nonionic osmolytes as a criterion to distinguish elements of the osmotic stress response from solute-specific responses. Nevertheless, in chemical terms, a limited range of solutes has been employed to impose osmotic stress. Furthermore, ProP (like other membrane-based osmosensors) is commonly exposed to a limited range of osmolytes in nature (*1*). Thus, even if ProP is designed to detect changes in extracellular osmolality, the osmosensory mechanism may be solute-specific and studies of its solute-specificity may be revealing. With the proteoliposome system, we can explore the solute specificity of ProP activation.

Recent efforts to systematically describe and explain water/solute/macromolecule interactions provide a useful context for this work [summarized by Wood (*1*)]. They suggest that solute specificity may exist in terms of the following: (A) the impact of the solutes on water structure (*23, 40*); (B) preferential interactions of the solute with the protein and/or the membrane surface (*41*); (C) the degree to which solutes are sterically excluded from water entrapped within the protein (*16*); and (D) the degree to which solutes are sterically excluded from the membrane, determining whether imposed osmotic upshifts cause changes in proteoliposome shape. Systematic effects of solutes (particularly electrolytes) on macromolecular structure and solubility have been correlated with their effects on water structure [creating the Hofmeister series, effect (A)]. Both steric [effect (C)] and other

constraints cause solutes to be excluded to various degrees from macromolecule/solvent interfaces, their exclusion being defined globally in terms of preferential interactions [effect (B)]. Increasing exclusion of solutes from macromolecular surfaces [effects (B) and (C)] favors conformations and interactions that minimize the solvent-exposed surface area for proteins and lipids. Interpretation of experimental data is challenging because real solutes simultaneously exert more than one of the effects listed above and the current literature falls short of establishing broadly accepted relationships and distinctions among them [e.g., (*42, 43*)].

In this paper, we report systematic analyses of the abilities of Hofmeister series anions and PEGs of varying molecular sizes to osmotically activate transporter ProP. The ability of a number of sodium salts to activate ProP-$(His)_6$ did not correlate with the position of the anion in the Hofmeister series (Figure 7). The lack of any systematic effect on ProP is in sharp contrast to the many well-documented effects of solutes from the Hofmeister series on the activity, solubility, and stability of soluble enzymes [reviewed in (*23, 40*)]. This difference may arise because membrane-bound ProP has less solvent-exposed surface area than soluble proteins. However, systematic Hofmeister effects on lipid membranes have also been reported. At concentrations as low as 0.5 M, kosmotropic and chaotropic solutes had opposite effects on the liquid-crystalline (L_α) to hexagonal (H_{II}) phase transition temperature of L-α-1-palmitoyl-2-oleoylphosphatidylethanolamine (POPE) liposomes (*24*). Relatively kosmotropic solutes favored the H_{II} phase which has the smaller area/lipid. Such an effect would be expected to increase the intrinsic curvature strain by increasing the headgroup (and acyl chain) proximity. Although lipid mixtures would be expected to behave differently than pure lipid, *E. coli* lipid (at 70% PE) may undergo qualitatively similar solute-induced changes in phase behavior as reported for POPE. Either ProP is unable to sense these changes in the lipid bilayer, lateral lipid phase separation mitigates changes in the ProP environment, the effects are too subtle to be measured, or other mutually compensatory effects on the protein and the membrane lipid yield no net manifestation.

At present, discussions of osmosensing by ProP and related systems are strongly influenced by the observed correlation between vesicle shrinkage and transporter activation. When a topologically closed membrane system such as a proteoliposome is exposed to an osmotic upshift with a membrane-impermeant osmolyte, lumenal water diffuses out until the osmotic gradient has collapsed. Since the compressibility of biological membranes is very limited (*44*), proteoliposomes subjected to an upshift will shrink and change shape to reduce their volume at essentially constant surface area (*33*). Vesicle shrinkage concentrates lumenal contents (increasing ionic strength as well as macromolecular crowding or confinement), and it may create local variations in membrane structure including lateral phase separation and changes in curvature strain. Such local membrane changes may be distinct in origin, if not in nature, from global effects of solvent osmolality on membrane structure. Concentration of the lumenal contents and alteration of membrane structure are among the perturbations that could activate ProP (Figure 1A) (*1*).

Before attempting to correlate ProP activation with any one consequence of proteoliposome shrinkage, we sought to determine whether shrinkage was essential. The activation of ProP by PEGs and other organic solutes may depend on their molecular size in two distinct ways. Their sizes determine their membrane permeabilities and hence their abilities to cause proteoliposome shrinkage. Their sizes also determine the degree to which they are excluded from the ProP protein, itself, and the size scales for these phenomena may differ. Since the osmotic activation of ProP cannot currently be detected in the absence of the membrane barrier, it is difficult to differentiate these effects.

The degrees of liposome shrinkage and ProP activation were determined after osmotic upshifts were imposed with glycerol, urea, and a series of poly(ethylene glycol)s (PEG) with molecular masses ranging from 62 to 1000 g/mol. All membrane-impermeant PEGs activated ProP-$(His)_6$ to similar extents at equivalent osmotic upshifts (Figures 4 and 8). Osmotic upshifts imposed with the membrane-permeant osmolytes glycerol, urea, PEG 62, and PEG 106 failed to activate ProP (Table 1 and Figure 8B). Importantly, however, upshifts imposed with the membrane-permeant compounds PEG 150 and PEG 200 caused small but reproducible activation of ProP-$(His)_6$. Thus, the molecular size scales for membrane permeability and ProP activation differed, and proteoliposome shrinkage was not essential for at least partial activation of ProP-$(His)_6$ (Figure 9).

Changes in preferential hydration, due to exclusion of added solutes from the macromolecular surface, can be the basis for conformational changes of macromolecules. In several studies, glycerol has been shown to be less excluded from protein surfaces than other solutes such as sucrose and betaine (*45, 46*). In their studies of hexokinase, Reid and Rand (*36*) found that PEGs of molecular weights less than 1000 were only partially excluded from an aqueous compartment around the protein. These authors concluded that PEG 1000 and larger molecules were sterically excluded from a cleft in the surface of hexokinase. Perhaps PEG 200 only partially activates ProP-$(His)_6$ because it is only partially excluded from the protein surface.

Our current data support at least two possible mechanisms of ProP activation. Surface dehydration may favor the active conformation of ProP. The degree of dehydration would be solute-dependent in that solutes that are more effectively excluded would cause greater dehydration and more complete activation. Alternatively, surface dehydration due to solute exclusion may only partially activate ProP because some other correlate of proteoliposomal shrinkage is required for full activation.

ACKNOWLEDGMENT

We are grateful to Joan Boggs, Wayne Bolen, Nola Fuller, Reinhard Krämer, Peter Rand, and the anonymous referees for helpful discussions and comments on the manuscript.

REFERENCES

1. Wood, J. M. (1999) *Microbiol. Mol. Biol. Rev. 63*, 230−262.
2. Csonka, L. N., and Hanson, A. D. (1991) *Annu. Rev. Microbiol. 45*, 569−606.
3. Strange, K. (1994) *Cellular and molecular physiology of cell volume regulation*, CRC Press, Boca Raton, FL.
4. Hanson, A. D. (1992) in *Water and Life: Comparative Analysis of Water Relationships at the Organismic, Cellular and Molecular Levels* (Somero, G. N., Osmond, C. B., and

Bolis, C. L., Eds.) pp 52−60, Springer-Verlag, Berlin, Heidelberg, and New York.
5. Timasheff, S. N. (1992) in *Water and Life: Comparative Analysis of Water Relationships at the Organismic, Cellular and Molecular Levels* (Somero, G. N., Osmond, C. B., and Bolis, C. L., Eds.) pp 70−84, Springer-Verlag, Berlin, Heidelberg, and New York.
6. Kempf, B., and Bremer, E. (1998) *Arch. Microbiol. 170*, 319−330.
7. Poolman, B., and Glaasker, E. (1998) *Mol. Microbiol. 29*, 397−407.
8. Booth, I. R., and Louis, P. (1999) *Curr. Opin. Microbiol. 2*, 166−169.
9. Grothe, S., Krogsrud, R. L., McClellan, D. J., Milner, J. L., and Wood, J. M. (1986) *J. Bacteriol. 166*, 253−259.
10. MacMillan, S. V., Alexander, D. A., Culham, D. E., Kunte, H. J., Marshall, E. V., Rochon, D., and Wood, J. M. (1999) *Biochim. Biophys. Acta 1420*, 30−44.
11. Culham, D. E., Lasby, B., Marangoni, A. G., Milner, J. L., Steer, B. A., van Nues, R. W., and Wood, J. M. (1993) *J. Mol. Biol. 229*, 268−276.
12. Racher, K. I., Voegele, R. T., Marshall, E. V., Culham, D. E., Wood, J. M., Jung, H., Bacon, M., Cairns, M. T., Ferguson, S. M., Liang, W.-J., Henderson, P. J. F., White, G., and Hallett, F. R. (1999) *Biochemistry 38*, 1676−1684.
13. Ruebenhagen, R., Roensch, H., Jung, H., Kraemer, R., and Morbach, S. (2000) *J. Biol. Chem. 275*, 735−741.
14. van der Heide, T., and Poolman, B. (2000) *Proc. Natl. Acad. Sci. U.S.A. 97*, 7102−7106.
15. Kaczorowski, G. J., and Kaback, H. R. (1979) *Biochemistry 18*, 3691−3697.
16. Parsegian, V. A., Rand, R. P., and Rau, D. C. (1995) *Methods Enzymol. 259*, 43−95.
17. Jansen, M., and Blume, A. (1995) *Biophys. J. 68*, 997−1008.
18. Zeidel, M. L., Ambudkar, S. V., Smith, B. L., and Agre, P. (1992) *Biochemistry 31*, 7436−7440.
19. Milner, J. L., Grothe, S., and Wood, J. M. (1988) *J. Biol. Chem. 263*, 14900−14905.
20. Kuznetsova, N., Rau, D. C., Parsegian, V. A., and Leikin, S. (1997) *Biophys. J. 72*, 353−362.
21. Parsegian, V. A., Rand, R. P., Colombo, M., and Rau, D. C. (1994) in *Biomembrane Electrochemistry* (Blank, M., and Vodyanoy, I., Eds.) pp 177−196, American Chemical Society, Washington, DC.
22. Leikin, S., Parsegian, V. A., Rau, D. C., and Rand, R. P. (1993) *Annu. Rev. Phys. Chem. 44*, 369−395.
23. Collins, K. D., and Washabaugh, M. W. (1985) *Q. Rev. Biophys. 18*, 323−422.
24. Sanderson, P. W., Lis, L. J., Quinn, P. J., and Williams, W. P. (1991) *Biochim. Biophys. Acta 1067*, 43−50.
25. Culham, D. E., Tripet, B., Racher, K. I., Voegele, R. T., Hodges, R. S., and Wood, J. M. (2000) *J. Mol. Recognit. 13*, 1−14.
26. Neidhardt, F. C., Bloch, P. L., and Smith, D. F. (1974) *J. Bacteriol. 119*, 736−747.
27. Jung, H., Tebbe, S., Schmid, R., and Jung, K. (1998) *Biochemistry 37*, 11083−11088.
28. Scopes, R. K. (1987) *Protein purification: principles and practice*, Springer-Verlag, New York.
29. Waggoner, A. S. (1979) *Methods Enzymol. 55*, 689−695.
30. Ramos, A., and Kaback, H. R. (1977) *Biochemistry 16*, 854−859.
31. Kendall, D. A., and MacDonald, R. C. (1983) *Anal. Biochem. 134*, 26−33.
32. Diehl, H. (1964) *Calcein, calmagite and o,o′-dihydroxyazobenzene. Titrimetric, colormetric, and fluorometric reagents for calcium and magnesium*, Frederic Smith Chemical Co., Columbus, OH.
33. White, G. F., Racher, K. I., Lipski, A., Hallett, F. R., and Wood, J. M. (2000) *Biochim. Biophys. Acta 1468*, 175−186.
34. Gennis, R. B. (1989) *Biomembranes: Molecular Structure and Function* Springer-Verlag, New York.
35. van der Heide, T., and Poolman, B. (2000) *J. Bacteriol. 182*, 203−206.
36. Reid, C., and Rand, R. P. (1997) *Biophys. J. 72*, 1022−1030.
37. Patel, L., Schuldiner, S., and Kaback, H. R. (1975) *Proc. Natl. Acad. Sci. U.S.A. 72*, 3387−3391.
38. Lever, M., Sizeland, P. C., Bason, L. M., Hayman, C. M., and Chambers, S. T. (1994) *Biochim. Biophys. Acta 1200*, 259−264.
39. Sizeland, P. C., Chambers, S. T., Lever, M., Bason, L. M., and Robson, R. A. (1995) *Am. J. Physiol. 268*, F227−F233.
40. Cacace, M. G., Landau, E. M., and Ramsden, J. J. (1997) *Q. Rev. Biophys. 30*, 241−277.
41. Timasheff, S. N. (1994) in *Protein−Solvent Interactions* (Gregory, R. B., Ed.) pp 445−482, Marcel Dekker, Inc., New York.
42. Timasheff, S. N. (1998) *Proc. Natl. Acad. Sci. U.S.A. 95*, 7363−7367.
43. Parsegian, V. A., Rand, R. P., and Rau, D. C. (2000) *Proc. Natl. Acad. Sci. U.S.A. 97*, 3987−3992.
44. Bloom, M., Evans, E., and Mouritsen, O. G. (1991) *Q. Rev. Biophys. 24*, 293−397.
45. Courtenay, E. S., Capp, M. W., Anderson, C. F., and Record, M. T., Jr. (2000) *Biochemistry 39*, 4455−4471.
46. Timasheff, S. N., and Arakawa, T. (1989) in *Protein Structure: A Practical Approach* (Creighton, T. E., Ed.) pp 331−345, IRL Press, Oxford.

BI002331U